

**Climate Change Initiative
Living Planet Fellowship**

2014

Jens Heymann

University of Bremen

4000112800/15/I-SBo

STANDARD COVER PAGE FOR ESA STUDY CONTRACT REPORTS

ESA STUDY CONTRACT REPORT		
ESA Contract No: 4000112800/15/I-SBo	SUBJECT: Partnership Agreement – The Living Planet Fellowship – CARBOn dioxide emissions from FIRES (CARBOFIRES)	CONTRACTOR: University of Bremen
ESA CR()No: 4000112800/15/I-SBo	No. of Volumes: 1 This is Volume No: 1	CONTRACTOR'S REFERENCE: University of Bremen, FB1, Institute of Environmental Physics (IUP), Bremen, Gemany
<p>ABSTRACT:</p> <p>Fires are an important source of atmospheric carbon dioxide (CO₂). Within the CARBOFIRES project CO₂ emissions from fires for several regions have been estimated using satellite XCO₂ retrievals and forward and inverse modelling. The most important burning regions on Earth are located in North and South Africa and in South America. The fires in these regions release large amounts of CO₂ into the atmosphere every year. Emission databases such as the Global Fire Emission Database (GFED4s) estimate the yearly global CO₂ emission to approximately 2000 MtC of which 400 MtC are released in North Africa, 700 MtC in South Africa, and up to 500 MtC in South America. These emissions were indirectly estimated by using parameters like burned area, fire radiative power, and emission factors. Within CARBOFIRES CO₂ emission in these regions were estimated more directly by using the column-averaged dry air mole fraction of CO₂, XCO₂, derived from measurements of the SCIAMACHY instrument onboard ENVISAT using GHG-CCI project XCO₂ retrievals. In the North Africa region, the estimated yearly CO₂ emission for the fire seasons between 2003 and 2011 is about 827±312 MtC, which is twice as much compared to GFED4s. The estimated yearly CO₂ emission for South Africa in this time period is about 452±244 MtC, which is about 36% smaller compared to the emission database. The CO₂ emission for South America is estimated to be about 289±143 MtC per year, which is similar to the emission database. Furthermore, the CO₂ emission of the year 2015 Indonesian fires has been estimated using OCO-2 XCO₂. The results have been published in Geophys. Res. Lett. (Heymann et al., 2017).</p>		
<p>The work described in this report was done under ESA Contract. Responsibility for the contents resides in the responsibility of the author.</p>		
<p>Names of author: Dr. Jens Heymann</p>		
<p>NAME OF ESA STUDY MANAGER: Dr. Stephen Plummer DIV: EOP-SC DIRECTORATE:EOP</p>	<p>ESA BUDGET HEADING:</p>	

Jens Heymann
CARBOFIRES

1 Introduction

Atmospheric carbon dioxide (CO₂) is the most important contributor to global warming [IPCC, 2013]. One of the most significant sources for atmospheric CO₂ is biomass burning. The global fire CO₂ emission amounts to approximately 2 GtCyr⁻¹ [van der Werf et al., 2010], which is about 25% of the anthropogenic fossil fuel emission (approximately 8 GtCyr⁻¹) [Canadel et al., 2007].

The CO₂ emissions from fires are primarily estimated by using indirect methods. The bottom-up emission inventory Global Fire Emissions Database (GFED) [van der Werf et al., 2010], for example, estimates emissions from parameters like burned area, fuel load, combustion completeness and emission factors. These parameters are obtained from satellite measurements, simulations, in-situ measurements and laboratory experiments.

The direct estimation of CO₂ emissions from measurements of the CO₂ concentration in fire regions requires an accurate and representative measurement of the increase in CO₂ attributable to the fire. For this purpose, in-situ measurement campaigns over fire regions were performed [Guyon et al., 2005, O'Shea et al., 2013]. However, the temporal and spatial restrictions of such campaigns provide only information from fires in a small area and for a limited time period.

Satellite observations, on the other hand, have a better spatial sampling, but have a lower accuracy compared to the in-situ measurements. Only very few studies basing directly on satellite CO₂ measurements have addressed the estimation of CO₂ emissions from fires. The main reason is that this is a challenging application because, due to large CO₂ background concentrations, even large forest fires are expected to enhance the CO₂ column (e.g., in units of molecules per unit area) only by a few per mill. However, this should be possible due to the latest significantly improved satellite-based CO₂ data sets which have been obtained, e.g., in the framework of ESA's GHG-CCI project [Hollmann et al., 2013, Buchwitz et al., 2015].

In this context, in European Space Agency's (ESA) Living Planet Fellowship project CARBOn dioxide emissions from FIRES (CARBOFIRES), CO₂ emissions of fires have been directly estimated by using satellite-derived CO₂ concentrations. In this document the results for the Indonesian fires in 2015 and the fire seasons in North and South Africa and South America are presented. Column-averaged dry air mole fraction of CO₂, XCO₂, data product retrieved from observations of NASA's Orbiting Carbon Observatory-2 (OCO-2) mission [Crisp et al., 2008; Crisp, 2015] and from observations of the SCanning Imaging Absorption spectromETER for Atmospheric CHartography (SCIAMACHY) on-board ESA's ENVironmental SATellite (ENVISAT) [Burrows et al., 1995, Bovensmann et al. 1999] have been used. To identify measurements affected by fires, atmospheric transport simulations have been performed by using the Stochastic Time-Inverted Lagrangian Transport model, STILT [Gerbig et al., 2003; Lin et al., 2003]. Observations unaffected by fires are used to define background concentrations in order to derive the XCO₂ enhancements related to the fire CO₂ emissions. The CO₂ emission is then subsequently estimated by comparing the XCO₂ enhancements with XCO₂ enhancements from the Copernicus Atmosphere Monitoring Service (CAMS) CO₂ analysis system implemented by the European Centre for Medium-Range Weather Forecast (ECMWF) [Massart et al., 2016], with model output from NOAA's global CO₂ modelling and assimilation system CarbonTracker [Peters et al., 2007] and with STILT model output.

2 Methods

The estimation of fire CO₂ emissions requires knowledge of how much of the XCO₂ column, retrieved from the satellite measurement, is affected by the fire emissions. This is a non-trivial task as the background XCO₂ values (XCO₂^{back}) are large (about 400 ppm) and variable and the expected XCO₂ enhancements related to fire CO₂ emissions (XCO₂^{fire}) are small (about 2 ppm for large fires). In order to determine the satellite XCO₂ enhancements, the difference between the satellite XCO₂ data (XCO₂^{obs}) and background XCO₂ values has been derived (XCO₂^{fire} = XCO₂^{obs} - XCO₂^{back}).

Three kinds of data sets are used for the estimation of fire CO₂ emissions from these satellite-based XCO₂ enhancements:

- Satellite CO₂ observations are used as main input for the analysis.
- Global CO₂ model is used for the determination of background CO₂ values, for inversions and for comparisons.
- Fire CO₂ emission inventory is used for the identification of fire regions, for inversions and for comparisons.

Figure 1 shows a schematic diagram of the methods used to estimate the fire CO₂ emission using these kinds of input datasets. The CO₂ emissions are estimated within three steps: The first step is the identification of fire affected satellite soundings. The second step is the determination of fire related XCO₂ enhancements. And the third step is the determination of a scaling factor for the CO₂ fire emission database. These three steps are described in the following sections.

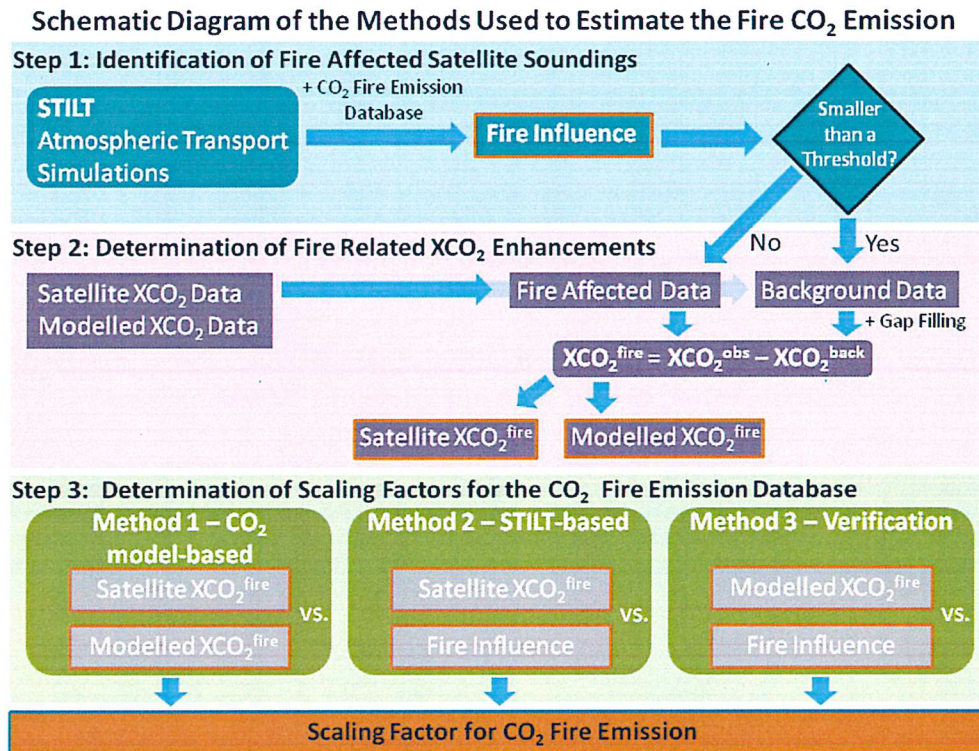


Figure 1. Schematic diagram of the methods used to estimate the satellite-based fire CO₂ emissions.

2.1 Determination of background CO₂ concentrations

The background XCO₂ data (XCO_2^{back}) have been constructed from satellite data, which are not influenced by fire CO₂ emissions, and a CO₂ model. An offset has been added to the model to minimize potential biases between the model and the satellite data. To what extent the satellite-derived XCO₂ is influenced by fire CO₂ emissions has been determined by atmospheric transport simulations performed by using the STILT model [Gerbig et al., 2003, Lin et al., 2003].

The STILT simulations have been performed in a manner similar to that described by Reuter et al. [2014]. Meteorological input for the simulations is taken from the ECMWF ERA Interim meteorology database [Berrisford et al., 2011]. Backwards trajectories starting at the location of the satellite measurement are computed for the previous 480 hours. The atmospheric column is split into 40 sub-layers, of which 25 are located in the planetary boundary layer. In the centre of each layer a (virtual) receptor is placed, which is the starting point of 25 particles. For each receptor a footprint is calculated, which represents the sensitivity of the receptor to surface fluxes, also called surface sensitivity. Unnecessary calculations are avoided by terminating particles, which leave a 10° bounding box around the area investigated. The vertical integration of the receptor footprints are performed by accounting for the column averaging kernels of the satellite XCO₂ retrievals. To

distinguish between fire affected and unaffected parts of the footprint, the footprints are multiplied with the fire CO₂ emission database. The resulting data field is called the fire influence. By integration over the fire region the accumulated fire influence of a sounding is calculated ($XCO_2^{\text{fire, STILT}}$), which represents the expected change of XCO₂ in ppm due to the fire CO₂ emission.

The satellite measurements, which are not influenced by fire CO₂ emissions, have been identified by small fire influences ($XCO_2^{\text{fire, STILT}} < \text{a threshold}$). The fire influences and satellite data have been gridded on daily grids to reduce the scatter of the satellite data and to reduce potential errors resulting from the atmospheric transport simulations. To obtain an error estimate of each grid cell, which is needed for the inversions, the variances of the measurement errors have been averaged within the grid cell (the measurement errors are assumed to be fully correlated within the grid boxes and for the day of measurement).

An offset has been added between the global CO₂ model, which is used to fill the gaps in the XCO₂ background fields, and the satellite XCO₂ background data to minimize potential regional biases in the model and satellite data. The CO₂ model used for this purpose is CarbonTracker. The CarbonTracker data do not only contain total XCO₂ fields but also the XCO₂ contribution fields from the biosphere, ocean, fossil fuel combustion, and from fires. In order to remove the fire signal in the CarbonTracker XCO₂ fields, the fire XCO₂ component fields are subtracted from the total XCO₂ fields. An offset between these model fields and the satellite background data has been added and the background XCO₂ fields have been sampled like the satellite data. These background XCO₂ concentrations (XCO_2^{back}) are then subtracted from the gridded fire affected satellite XCO₂ data (XCO_2^{obs}) to obtain the fire related XCO₂ enhancements ($XCO_2^{\text{fire}} = XCO_2^{\text{obs}} - XCO_2^{\text{back}}$).

2.2 Estimation of fire CO₂ emissions

The fire CO₂ emissions are estimated from the fire related XCO₂ enhancements by using two approaches. The first approach estimates the emission by a comparison of the satellite based XCO₂ enhancements with corresponding model XCO₂ enhancements ($XCO_2^{\text{fire, model}}$), which are determined by using the identical sampling as the satellite data and the same method to find the background concentrations. The global CO₂ model incorporates emissions from a fire emission inventory for the modelling of the XCO₂ fields. Thus, the ratio of the XCO₂ enhancements provides a scaling factor for the fire CO₂ emissions provided by these inventories. A linear relationship is assumed. This method is referred to as "CO₂ model-based estimation method" (CM) in the following.

The second approach uses the STILT-based fire influences to estimate the fire CO₂ emissions. The STILT fire influences ($XCO_2^{\text{fire, STILT}}$) are calculated by multiplication of the surface sensitivity with the fire CO₂ emissions of an emission inventory. Consequently, the scaling factor between the satellite XCO₂ enhancements and the fire influence can also directly be interpreted as a scaling of the fire CO₂ emission database. This method is referred to as "STILT-based estimation method" (SM) in the following.

The inversion method used to estimate the scaling factor between the satellite and model enhancements is maximum likelihood. The following cost function has been minimized.

$$\chi = (\mathbf{y} - \mathbf{F}(\mathbf{x}))^T \mathbf{S}_\varepsilon^{-1} (\mathbf{y} - \mathbf{F}(\mathbf{x}))$$

The state vector \mathbf{x} consists of a scaling factor (x_{scale}) and an offset (x_{offset}). The offset reduces biases between the background concentrations and the fire-affected satellite data.

The measurement vector \mathbf{y} contains all satellite XCO₂ enhancements. The forward model \mathbf{F} is represented by the model XCO₂ enhancements or the STILT fire influences depending on the estimation method (e.g., for the CO₂ model-based estimation method $\mathbf{F}(\mathbf{x}) = x_{\text{offset}} + x_{\text{scale}} \cdot \mathbf{XCO}_2^{\text{fire, model}}$). The measurement error covariance matrix \mathbf{S}_ε is constructed from the root sum square (square root of the sum of the variances) of the satellite measurement uncertainty and an estimate of the uncertainty of the fire emission database. For the CO₂ model-based method, an estimate of the model uncertainty has been added.

The uncertainty resulting from the emission database has been estimated assuming a linear error parameterization. This error parameterization accounts for uncertainties resulting from the emission estimate of the database, as well as uncertainties attributed to the spatial pattern of the emissions. This is needed

because the CO₂ model-based and STILT-based estimation methods depend on this pattern. The linear error parameterization is as follows

$$\Delta\text{INV} = b_0 + b_1 \cdot \text{INV},$$

where INV is the gridded emission inventory and ΔINV the gridded estimated uncertainty of the fire CO₂ emission database. The b_0 term provides an error estimate for grid cells, including those with no emissions and has been estimated by using the 50% percentile of all fire CO₂ emissions in the region of interest excluding zero emissions. The b_1 term has been assumed to be 1. Thus, the fire emission is assumed to have an uncertainty of more than 100%, which is a conservative assumption. The uncertainty resulting from the emission database has then been estimated by the same method as used to compute the STILT fire influences. ΔINV has been multiplied with the STILT footprints and spatially integrated, i.e., the error analysis is based on replacing the emission inventory by ΔINV . The contribution to the posteriori uncertainty of the scaling factor is small and is dominated by the satellite measurement uncertainty.

The minimization of the cost function results in the a posterior solution \hat{x} :

$$\hat{x} = x_0 + \hat{S}[K^T S_\varepsilon^{-1}(y - F(x_0))]$$

$$\hat{S} = (K^T S_\varepsilon^{-1} K)^{-1}$$

The covariance matrix \hat{S} is used to calculate the a posterior errors. K is the Jacobian matrix, which is derived from either the model XCO₂ enhancements or the STILT fire influences. x_0 is the first guess and is set (for the scaling factor as well as for the offset) to 0.

The results presented here are based on gridded data. All uncertainties correspond to 1-sigma unless otherwise noted.

3 Indonesian fires in 2015

An extensive fire season in Indonesia has greatly contributed to the global CO₂ fire emissions in 2015. These fires were a consequence of decades of drying of peatland and forest clearing, which led to a high flammability of the landscape [Wooster et al, 2012, Field et al, 2008]. An El Niño event, which is associated with droughts, intensified this situation.

Most of the affected fire regions in Indonesia were located on Kalimantan, Sumatra, and Papua, where the fire season had its strongest intensity between August and October 2015 [Huijnen et al., 2016]. During this time period, the large release of air pollutants compromised the air quality and influenced the health of the population [Marlier et al., 2013, Tacconi, 2016]. Open fires together with smouldering and underground burning of the landscape, especially of the carbon-rich peatland, contributed to large carbon emissions [Huijnen et al., 2016]. The fire season ended with the onset of heavy rains over Kalimantan at the end of October 2015.

According to the Global Fire Assimilation System (GFASv1.2) [Kaiser et al., 2012] the Indonesian fires released about 1157 MtCO₂ between July and November 2015. This emission is larger compared to that estimated (1064 MtCO₂) in the Global Fire Emission Database (GFED4s) [van der Werf et al., 2010]. Most of the CO₂ was emitted within the main fire period from September to October 2015 (GFASv1.2: 945 MtCO₂; GFED4s: 851 MtCO₂). These emissions have been derived indirectly from parameters such as burned area, fire radiative power, and emission factors, which have been obtained from satellite, in-situ and laboratory measurements.

An alternative approach to determine fire CO₂ emissions employs satellite data of co-emitted species such as CO. CO fire emissions are determined from these observations and multiplied by CO to CO₂ emission factors. This also indirectly yields in estimates of fire CO₂ emissions. Huijnen et al. [2016] applied this method to the Indonesian fires for the main fire period from September to October 2015. They found a fire CO₂ emission for this time period of about 692±213 MtCO₂.

In the CARBOFIRES project, the fire CO₂ emission for the Indonesian fires in 2015 has been estimated from the column-averaged dry air mole fraction of CO₂, XCO₂, data product retrieved from observations of NASA's

Orbiting Carbon Observatory-2 (OCO-2) mission [Crisp et al., 2008, Crisp, 2015]. The results of this activity have been published [see Heymann et. al, 2017]. In the following, the datasets used and the results for the Indonesian fires in 2015 are presented.

3.1 Datasets used

The satellite XCO₂ observations used to estimate the fire CO₂ emissions are obtained from the OCO-2 mission [Crisp et al., 2008, Crisp, 2015] launched on 2 July 2014. OCO-2 provides measurements with a spatial resolution of <1.3 km × 2.25 km. The algorithm used to retrieve XCO₂ from the satellite observations has been described by O'Dell et al. [2012] and Crisp et al. [2012]. For this study, about 134,000 individual OCO-2 XCO₂ retrievals of product version 701r from the time period July to November 2015 are used as input for our analysis. The only other available XCO₂ observations in this time period are based on GOSAT. Unfortunately, the amount of XCO₂ data based on GOSAT is too limited in this time period and in the Indonesian region for the estimation of fire CO₂ emissions.

A CO₂ fire emission database has been used for the identification of measurements affected by fires. Furthermore, the developed methods used to estimate the fire CO₂ emissions are based on a scaling of the CO₂ emission of this inventory. The database used for the Indonesian fires in 2015 is ECMWF's GFAS version 1.2 [Kaiser et al., 2012] (available from <http://apps.ecmwf.int/datasets/data/cams-gfas/>). GFASv1.2 uses the fire radiative power data product of MODIS and derives biomass combustion rates. The CO₂ emissions are obtained by applying emission factors to the biomass combustion rates. GFASv1.2 provides daily global CO₂ fire emissions with a spatial resolution of 0.1°×0.1°. In addition to GFASv1.2, the GFED version 4s database has been used for comparisons [van der Werf et al., 2010].

In addition to the satellite XCO₂ observations and the CO₂ emission databases, a global CO₂ model dataset is used. The satellite data have been compared with the model to estimate the fire CO₂ emission. Furthermore, an error analysis has been performed using the model CO₂ dataset. For this purpose, data from the CAMS ECMWF CO₂ analysis system has been used and is referred to as "CAMS CO₂ model" in the following [Massart et al., 2016]. The CO₂ analysis system assimilates satellite CO₂ observations from the GOSAT BESD XCO₂ algorithm [Heymann et al., 2015]. The underlying model uses fire emissions from GFASv1.2, and it has a spatial resolution of 80 km × 80 km and a temporal resolution of 3 hours. The amount of assimilated GOSAT data in the Indonesian region for the time period investigated is very limited. Consequently, the influence of the assimilated satellite data on the fire CO₂ signal is expected to be negligible. For the CO₂ model-based method, an estimate of the CAMS model uncertainty (1.2 ppm) has been added obtained from the validation study performed by Massart et al. [2016]. Besides the CAMS CO₂ model, NOAA's modelling and assimilation system CarbonTracker (CT-NRT obtained from <http://carbontracker.noaa.gov>) [Peters et al., 2007] has been used for the determination of the background concentrations to derive fire related XCO₂ enhancements needed to estimate the CO₂ emissions.

3.2 Results and error analysis

Figure 2 shows the OCO-2 XCO₂ data (XCO_2^{OCO-2}), the used background concentrations (XCO_2^{back}) and the XCO₂ enhancements (XCO_2^{fire}) for the Indonesian region in the time period from July to November 2015. The spatial distribution of the satellite observations shows that most of the measurements used are performed over the ocean as high quality XCO₂ data in the direct vicinity of fires are challenging to obtain due to high loads of smoke and aerosols. However, the observations over ocean can contain a substantial amount of information about the fires as the observed air masses can be affected by these fires (depending on wind direction). As can be seen, the subtraction of the background concentration from the OCO-2 XCO₂ results in XCO₂ enhancements of up to 2 ppm.

The OCO-2 measurements, which are not influenced by fire CO₂ emissions, have been identified by small fire influences ($XCO_2^{fire, STILT} < 0.001$ ppm). This results in ~70,000 OCO-2 background and ~64,000 fire affected observations. The OCO-2 data and the corresponding fire influences have been gridded on daily 0.5°×0.5° grids (see e.g. Fig. 2 for OCO-2 XCO₂, background XCO₂ and the resulting XCO₂ enhancements) to reduce the scatter of the satellite data and to reduce potential errors resulting from the atmospheric transport simulations. The bounding box around the investigated area covers the latitude range between -12° and 7° and the longitude range between 93° and 142°.

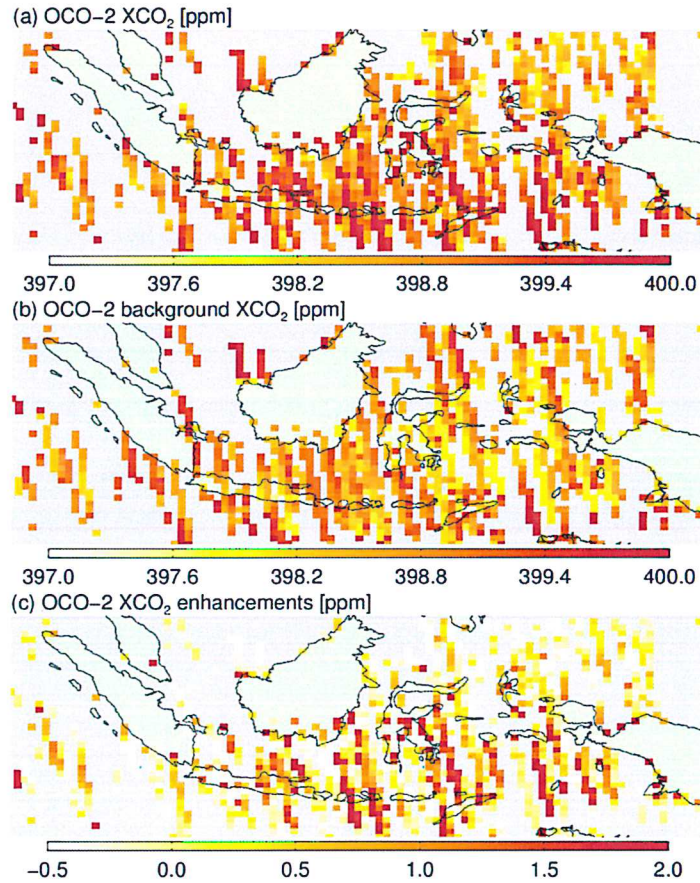


Figure 2. (a) OCO-2 XCO₂, (b) corresponding background XCO₂, and (c) XCO₂ enhancements on a 0.5°×0.5° grid for the Indonesian region (Lat: -12° - 7°; Lon: 93° - 142°) and the time period July to November 2015.

The CO₂ emissions for the Indonesian fires have been estimated by using the CO₂ model-based and the STILT-based estimation methods. Figure 3 shows the result of these methods. The fitted scaling factors are similar for both, the STILT-based method (0.63) and the CO₂ model-based method (0.66). The scaling factors are smaller than one showing that the satellite-based fire CO₂ emission is smaller than the GFASv1.2 emission.

Figure 4 shows the spatial distribution of the CO₂ emissions as well as the estimated satellite-based emissions, which are also summarised in Tab. 1. The STILT-based method results in an emission of 729±226 MtCO₂ and the CO₂ model-based method results in an emission of 766±191 MtCO₂. On average the OCO-2 based CO₂ fire emission in Indonesia is about 748±209 MtCO₂ (assuming correlated errors of the emissions) for the period from July to November 2015 which is 35% lower compared to GFASv1.2 (1157 MtCO₂) and 30% lower compared to GFED4s (1064 MtCO₂). This result is consistent with the corresponding value in the recently updated version GFASv1.3 (937 MtCO₂; Kaiser et al. [2016]). And it is even closer to the result of Huijnen et al. [2016] (they used GFAS output but with different emission factors), who also found lower emissions than the fire emission databases, albeit for the period from September to October 2015 (27% lower than GFASv1.2 and 19% lower than GFED4s).

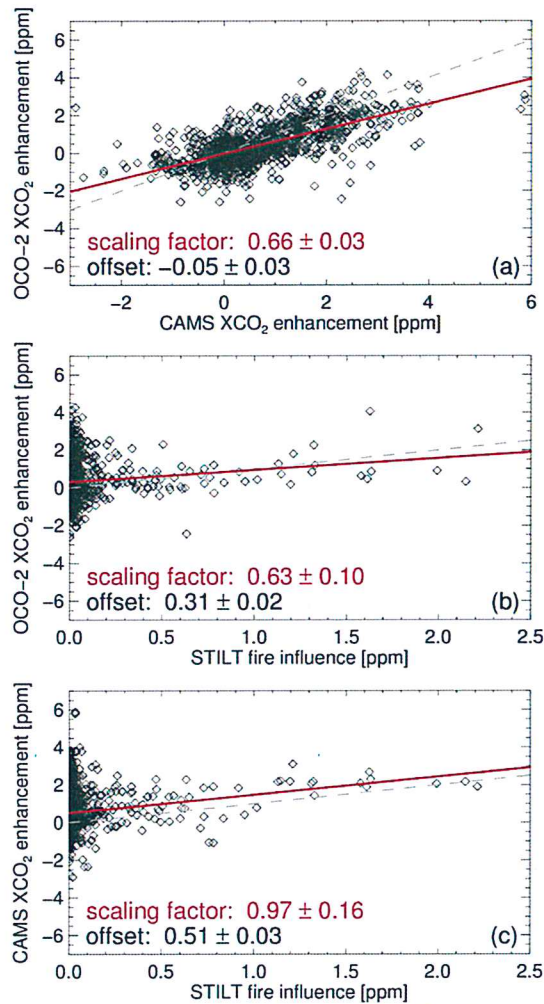


Figure 3. The results of the comparison between (a) OCO-2 and CAMS XCO₂ enhancements, (b) OCO-2 XCO₂ enhancements and STILT fire influences, and (c) CAMS XCO₂ enhancements and STILT fire influences. The gray dashed lines are the 1:1 lines and the red lines indicate the fitted offset and scaling factors.

Estimated CO₂ emission for the 2015 Indonesian fires (July - November)

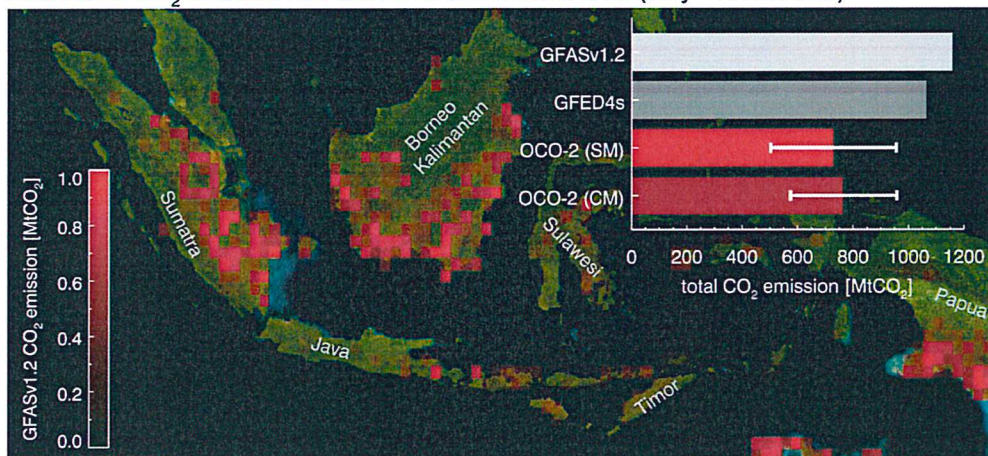


Figure 4. Estimated CO₂ emissions for the Indonesian fires in the time period from July to November 2015 (bars to the right) based on OCO-2 (red, dark red) compared to the GFASv1.2 (light grey) and GFED4s emissions (dark grey). The OCO-2 emissions are obtained by using the STILT-based method (SM, shown in red) and by using the CO₂ model based method (CM, shown in dark red). Shown is also the spatial distribution of the fire CO₂ emissions based on GFASv1.2.

	CO ₂ emission [MtCO ₂]
GFASv1.2	1157
GFED4s	1064
OCO-2 (SM)	729±226
OCO-2 (CM)	766±191
CAMS (SM)	1117±183

Table 1. Estimated CO₂ emissions for the Indonesian fires for the time period from July to November 2015. The OCO-2 based emissions are obtained by using the STILT-based method (SM) and the CO₂ model-based method (CM). The CO₂ emission based on the CAMS XCO₂ enhancements is obtained by using the STILT-based method (SM).

In order to estimate the uncertainty of the derived emissions, an error analysis has been performed. For this purpose, the STILT-based estimation method has been applied to the CAMS XCO₂ enhancements. The CAMS enhancements are obtained by using the same methods as those used for the satellite data, i.e. same sampling and use of the same method to determine the background concentrations. As the underlying model of the CAMS analysis system uses the GFASv1.2 fire CO₂ emissions as input, and STILT fire influences are computed by using also the GFASv1.2 emissions, a scaling factor of 1 between the data sets should be expected.

As shown by Fig. 3, a scaling factor of 0.97 ± 0.16 , which is close to 1, verifies the STILT-based estimation. The systematic difference of the scaling factor to the expected scaling factor is 3%, which has been used as an estimate for the systematic uncertainty of the scaling factor. The systematic difference is related to background (e.g., the used offset between CarbonTracker and the OCO-2 background values), sampling and atmospheric transport errors. These error sources also contribute to the statistical uncertainty. To obtain an estimate for this, the uncertainty found for the scaling factor of 16% has been used.

Another error component is related to the satellite data uncertainty, which is considered together with the goodness of the fit and the assumed GFASv1.2 uncertainty in the a posteriori error of the inversion result. For the STILT-based method an uncertainty of 15% and for the CO₂ model-based method an uncertainty of 5% were found.

Other error sources include potential biases in the satellite data, which are correlated with the fire influence. Most of these biases only contribute to the scatter of the satellite enhancements, i.e. they influence the goodness of the fit. Especially the large amount of co-emitted aerosols can potentially cause retrieval biases. In order to estimate how strong the influence of aerosol related biases in the OCO-2 XCO₂ data is, the difference between the OCO-2 and CAMS model XCO₂ is compared with CAMS based aerosol optical depth (AOD) at 550 nm (available from <http://apps.ecmwf.int/datasets/data/macc-nrealtime/>, data from Aerosol-CCI are not used because the time period investigated is not available). It is assumed that the difference between the satellite and analyzed XCO₂ is an estimate for the systematic error of the satellite data. It has to be noted that a correlation between the XCO₂ enhancements used for the estimation of the fire CO₂ emissions and aerosols is expected as fires are also a source of aerosols. In addition to the aerosols, the surface albedo was investigated. A surface albedo at 858 nm is used, which is based on the MODIS land surface black-sky albedo (available from <http://modis-atmos.gsfc.nasa.gov/ALBEDO/index.html>). As can be seen in Fig. 5 virtually no correlations have been found: $r = -0.06$ for AOD and $r = 0.03$ for albedo (no bias between observations over land, high albedo, and ocean, low albedo, has been found).

Despite the very low correlations, the impact of aerosol and albedo related errors in the satellite data on the estimated fire CO₂ emissions has been estimated by using a linear bias correction scheme for the satellite XCO₂ data. The coefficients for the linear bias correction are determined by a linear fit between the AOD/albedo and the XCO₂ difference. The bias corrected data set was then used to estimate the fire CO₂ emissions. The systematic errors resulting from aerosol and albedo related biases are estimated from the difference between the estimated emissions based on bias-corrected and non-bias-corrected satellite XCO₂ enhancements. The systematic error due to biases related to the albedo is less than 0.2%. For aerosols, the estimated error contribution is less than 4%.

A summary of the different errors contributing to the overall uncertainty is shown in Tab. 2. The uncertainty for the STILT-based method (31%) is slightly larger compared to the CO₂ model-based method (25%). These overall uncertainties have been computed from the root sum square (square root of the sum of the variances of the

errors) of the overall statistical and the sum of all systematic errors. The overall statistical error has been computed from the individual statistical errors by the root sum square.

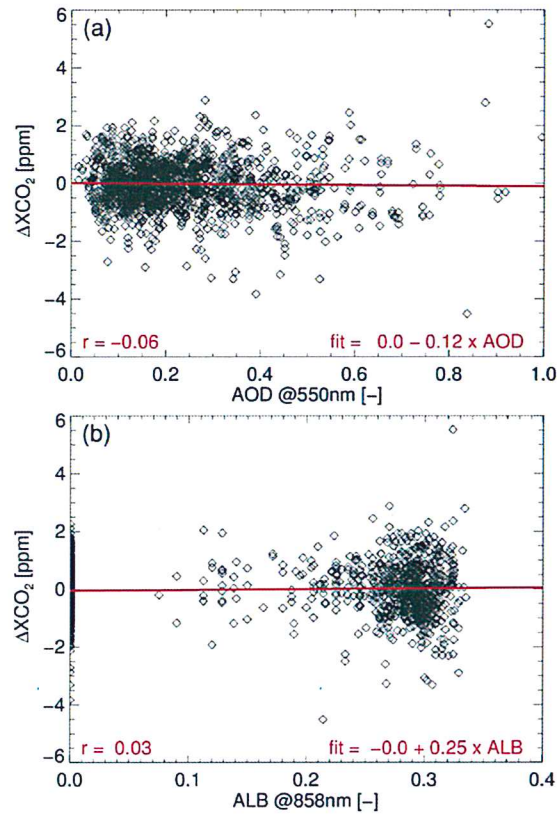


Figure 5. (a) Scatter plot of OCO-2 minus CAMS model XCO₂ (Δ XCO₂) versus CAMS AOD at 550 nm and (b) Δ XCO₂ versus MODIS-based surface albedo at 858 nm. The red lines indicate the linear fits between the data sets. In the bottom of each panel the correlation coefficient (r) and the fit parameters are shown. As can be seen, the correlations are very small, indicating that Δ XCO₂ is not significantly affected by aerosols and albedo related retrieval errors.

Error Contribution	SM		CM	
	Systematic	Statistical	Systematic	Statistical
Data and GFASv1.2 uncertainty	-	0.095	-	0.029
Background, sampling, atmospheric transport	0.034	0.159	0.034	0.159
Aerosols	0.028	-	0.005	-
Albedo	-0.001	-	-0.0004	-
All	0.063	0.185	0.0394	0.162
Overall	0.195 (31 %)		0.166 (25.1 %)	

Table 2. Error analysis results for the scaling factor obtained by using the STILT-based estimation method (SM) and the CO₂ model-based estimation method (CM).

4 North and South African, and South American fire seasons

The most important burning regions on Earth contributing to the global fire CO₂ emissions are located in North and South Africa (Northern and Southern of the equator) and in South America (especially Brazil) [Duncan et al., 2003]. The high demand for food and space for a growing population made the mankind the most important source of fires in these regions [Archibald et al., 2012]. However, human beings are not the only ignition sources as lightning and volcanoes can also introduce uncontrolled wildfires over large regions affecting the ecosystem [Bowman et al., 2009].

In the North Africa region, the fire season is typically between autumn and spring (Sep. – May). According to GFED4s about 400 MtC (~1440 MtCO₂) are emitted in this region into the atmosphere every year. The fire season in South Africa is typically between May and November and about 700 MtC (~2520 MtCO₂) are emitted in a year. In South America the fire season is typically between April and October. The year-to-year variation of the CO₂ emission in this region is larger as compared to the other regions and varies between about 100 MtC (in 2009, ~360 MtCO₂) and 500 MtC (in 2010, ~1800 MtCO₂).

Within the CARBOFIRES project, the fire CO₂ emissions for these regions have been estimated by using satellite-based XCO₂ retrieved from measurements of the SCIAMACHY instrument [Burrows et al., 1995, Bovensmann et al. 1999] onboard ENVISAT. In the following, the datasets used and the results for the analysis of these regions are presented.

4.1 Datasets used

The satellite XCO₂ observations are based on the BESD retrieval algorithm, which has been developed at the University of Bremen to retrieve XCO₂ from SCIAMACHY nadir measurements [Reuter et al., 2010; Reuter et al., 2011]. The algorithm is a core algorithm within ESA's Climate Change Initiative (CCI) [Hollmann et al., 2013, Buchwitz et al., 2015, Dils et al., 2014] aiming at delivering high quality satellite retrievals. A detailed description of BESD can be found in the Algorithm Theoretical Basis Document (ATBD) [Reuter et al., 2015] (available at <http://www.esa-ghg-cci.org/>). Here, the SCIAMACHY BESD product version 02.01.02 is used. The data set consists of individual satellite measurements, i.e. Level 2 data, and covers the time period 2003 – 2012. A validation study using TCCON data shows that the SCIAMACHY BESD XCO₂ data product has a station-to-station bias deviation of 0.39 ppm and a precision of 1.91 ppm (Comprehensive Error Characterisation Report – BESD, Reuter et al. [2016], available at <http://www.esa-ghg-cci.org/>; similar results have been found by Heymann et al. [2015] but for the previous version of SCIAMACHY BESD).

The fire CO₂ emission database used for the estimation of the fire CO₂ emission in the North and South Africa, and South America region is the Global Fire Emissions Database (GFED) version 4s (download from <http://www.globalfiredata.org>) [van der Werf et al., 2010] as the fire CO₂ emissions in CarbonTracker are based on GFED. The GFED4s data set has a temporal resolution of 3 hours and a spatial resolution of 0.25°x0.25°.

The global CO₂ model dataset used here is NOAA's global CO₂ modelling and assimilation system CarbonTracker, which has been developed to estimate CO₂ surface fluxes and corresponding CO₂ concentrations [Peters et al., 2007]. The CarbonTracker model includes atmospheric transport and considers for photosynthesis and respiration, the sea-air exchange and the CO₂ released from fires and from the combustion of fossil fuels. Fire emissions are account for by using a fire emission inventory. Within the assimilation process, the model results of CarbonTracker are compared with the CO₂ measurements from NOAA's air sampling network. The differences are interpreted as differences from the a-priori model fluxes to the real fluxes. The adaptation of the model fluxes to the observations leads typically to improved and less uncertain fluxes. CarbonTracker version CT2015 has been used (download from <http://carbontracker.noaa.gov>) for the time period 2003 to 2012. The model has a spatial resolution of 3°x2°.

4.2 Results and error analysis

The fire CO₂ emissions have been estimated for all full years covered by the SCIAMACHY BESD XCO₂ dataset, i.e., 2003 to 2011. The both introduced methods, the CO₂ model-based estimation method and the STILT-based estimation method, have been used to estimate the satellite-based fire CO₂ emission in the regions North and South Africa and South America. In the following the results and error analysis for the fire CO₂ emissions in these regions are presented.

4.2.1 North Africa

Figure 6 shows the averaged SCIAMACHY XCO₂ data (XCO₂^{obs}), the used background concentrations (XCO₂^{back}) and the XCO₂ enhancements (XCO₂^{fire}) for North Africa (northern of the equator) for the fire seasons 2003/2004 (Sep. – May) to the season of 2011/2012. The spatial distribution of the satellite observations shows that the subtraction of the background concentration from the SCIAMACHY XCO₂ results in XCO₂ enhancements of up to 5 ppm.

The SCIAMACHY measurements, which are not influenced by fire CO₂ emissions, have been identified by small fire influences ($XCO_2^{fire, STILT} < 0.01$ ppm). The SCIAMACHY data and the corresponding fire influences have been gridded on daily 1°x1° grids (see e.g. Fig. 6 for SCIAMACHY XCO₂, background XCO₂ and the resulting XCO₂ enhancements) to reduce the scatter of the satellite data and to reduce potential errors resulting from the atmospheric transport simulations. The bounding box around the investigated area covers the latitude range between 0° and 35° and the longitude range between -18° and 48°.

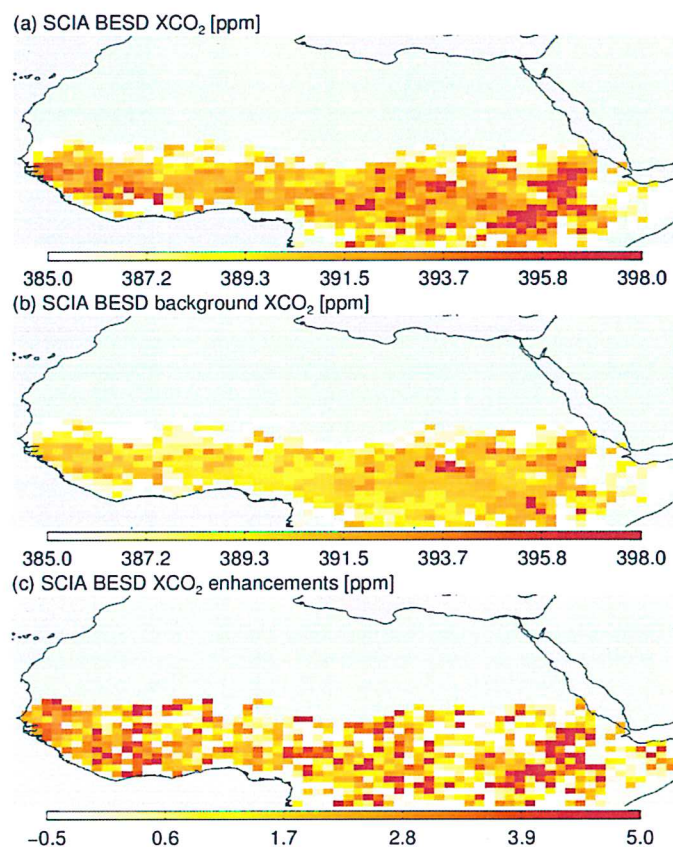


Figure 6. (a) SCIAMACHY BESD XCO₂, (b) corresponding background XCO₂, and (c) XCO₂ enhancements on a 1°x1° grid for North Africa and averaged over the fire seasons (Sep. – May) 2003/2004 to 2011/2012.

Figure 7 shows the estimated fire CO₂ emissions based on the CO₂ model-based method and the STILT-based method. The satellite-based CO₂ emissions are typically larger compared to the GFED4s emissions (shown by the green and dark green bars in Fig. 7). Especially the fire season of 2004/2005 and the fire season of 2006/2007 are larger compared to GFED4s. The blue bars show the estimated emissions of the CarbonTracker XCO₂ enhancements using the STILT-based method. Here, similar emissions as compared to GFED4s are expected as CarbonTracker uses the fire CO₂ emissions of GFED as input. Reasons for the large difference of the CarbonTracker based emissions especially in the season 2008/2009 can be an insufficient sampling as well as large uncertainties in the atmospheric transport in this time period. These can also be the reasons for the large difference between the satellite-based emissions for the different estimation methods (SM and CM) in this fire season.

Table 3 summarizes the found CO₂ emissions. The satellite-based CO₂ emissions are in most seasons nearly a factor of 2 larger compared to the emission inventory. The emissions averaged and the standard deviation for the different methods show that the results of the STILT-based method (SM) are more variable (mean CO₂ emission: 806±422MtC) than the results of the CO₂-model based method (CM, mean CO₂ emission: 848±312 MtC). The reason for this can be larger uncertainties in the atmospheric transport performed by STILT as compared to the CO₂ model. Overall, the estimated emission for all years using both methods is 827±312 MtC, which is about 96 % larger compared to GFED4s.

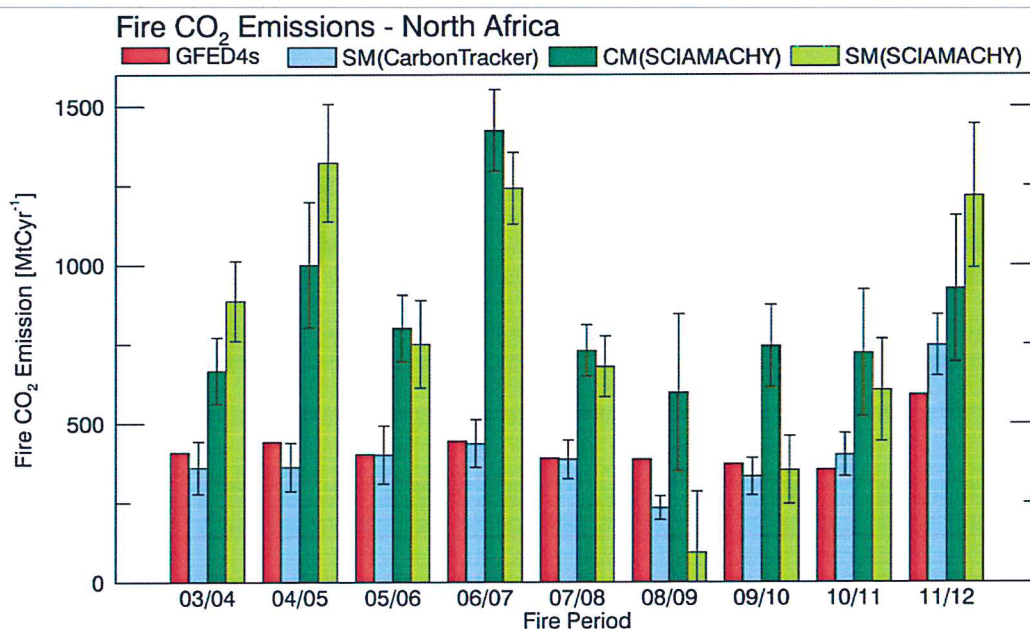


Figure 7. Estimated CO₂ emissions for fire seasons between 2003/2004 to 2011/2012 in North Africa based on SCIAMACHY BESD (green, dark green) compared to the GFED4s (red). The SCIAMACHY emissions are obtained by using the STILT-based method (SM, shown in green) and by using the CO₂ model based method (CM, shown in dark green). The emissions shown in blue are obtained by using the STILT-based method for the CO₂ model fire enhancements.

Fire season	CO ₂ Emission [MtC]			
	GFED4s	SM	CM	Mean
03/04	409	889±125	666±105	778±115
04/05	443	1325±185	996±196	1160±191
05/06	402	756±139	802±105	778±123
06/07	446	1243±110	1417±128	1330±119
07/08	391	690±101	728±82	709±92
08/09	387	94±192	598±248	346±222
09/10	372	363±106	751±126	557±116
10/11	355	632±182	736±229	684±207
11/12	592	1260±264	933±252	1097±258
Mean	422±70	806±422	848±247	827±312

Table 3. Estimated CO₂ emissions for fire seasons in North Africa. The SCIAMACHY BESD based emissions are obtained by using the STILT-based method (SM) and the CO₂ model-based method (CM). Mean values and their standard deviation for all fire seasons are shown in the bottom. The mean values on the right are the means of the SM and CM based emissions.

The error analysis for the estimated fire CO₂ emissions has been performed similarly to the Indonesian fire in 2015. The influence of aerosol and albedo related biases in the satellite data on the estimated emissions has been determined by the investigation of correlations of the difference between SCIAMACHY BESD and CarbonTracker XCO₂, which is regarded as an estimation of the systematic error of the satellite data, with aerosol and albedo related data. For aerosols the Aerosol Optical Depth (AOD) at 550 nm based on the MACC reanalysis database available from <http://apps.ecmwf.int/datasets/data/macc-reanalysis/levtype=sfc/> has been used. For the albedo the surface albedo at 858 nm is used, which is based on the MODIS land surface black-sky albedo available from <http://modis-atmos.gsfc.nasa.gov/ALBEDO/acquiring.html>. The results of this analysis have been summarized in Tab. 4 for the fire season 2003/2004. The overall uncertainty is in this time period for the STILT-based method about 14 % (1σ) and for the CO₂ model-based method about 16 % (1σ).

Error Contribution	SM		CM	
	Systematic	Statistical	Systematic	Statistical
Data and uncertainty	-	0.195	-	0.100
Background, sampling, atmospheric transport	0.118	0.202	0.118	0.202
Aerosols	0.001	-	10^{-6}	-
Albedo	0.003	-	0.002	-
All	0.121	0.281	0.120	0.225
Overall	0.306 (14.1 %)		0.255 (15.7 %)	

Table 4. Error analysis results for the scaling factor obtained by using the STILT-based estimation method (SM) and the CO₂ model-based estimation method (CM) for the North African fire season in 2003/2004.

4.2.2 South Africa

The SCIAMACHY XCO₂ data (XCO_2^{obs}), the used background concentrations (XCO_2^{back}) and the XCO₂ enhancements (XCO_2^{fire}) for South Africa (southern of the equator) averaged over the fire season in 2003 (May - November) to the season in 2011 are shown in Fig. 8. The spatial distribution of the satellite observations shows that the subtraction of the background concentration from the SCIAMACHY XCO₂ results in XCO₂ enhancements of up to 4 ppm.

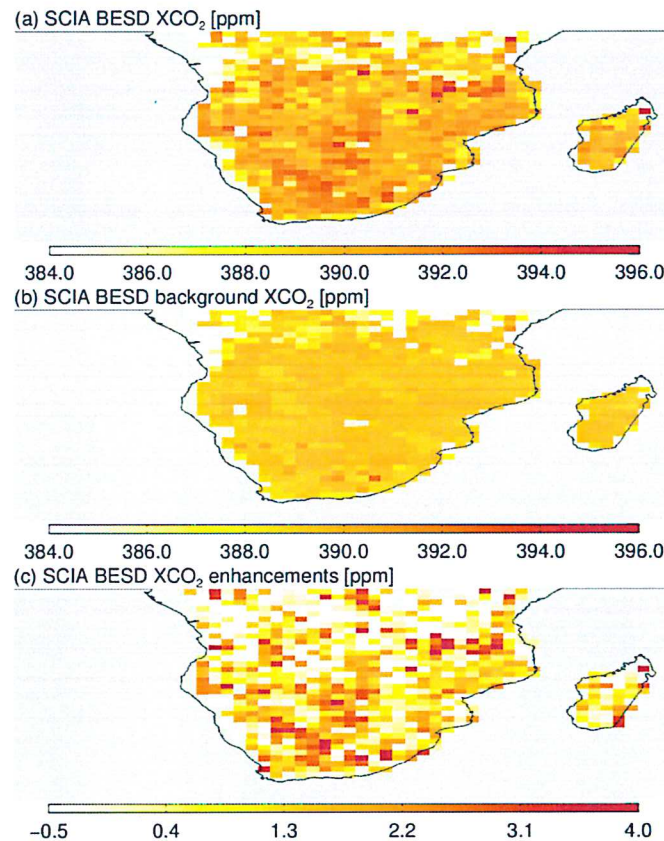


Figure 8. (a) SCIAMACHY BESD XCO₂, (b) corresponding background XCO₂, and (c) XCO₂ enhancements on a 1°×1° grid for South Africa and averaged over the fire seasons 2003 to 2011.

The SCIAMACHY measurements, which are not influenced by fire CO₂ emissions, have been identified by small fire influences ($XCO_2^{fire, STILT} < 0.01$ ppm). The SCIAMACHY data and the corresponding fire influences have been gridded on daily 1°×1° grids (see Fig. 8 for SCIAMACHY XCO₂, background XCO₂ and the resulting XCO₂ enhancements) to reduce the scatter of the satellite data and to reduce potential errors resulting from the

atmospheric transport simulations. The bounding box around the investigated area covers the latitude range between -38° and 0° , and the longitude range between -2° and 52° .

Figure 9 shows the estimated fire CO₂ emissions based on the CO₂ model-based method and the STILT-based method. The satellite-based CO₂ emissions are similar or smaller compared to the GFED4s emissions (shown by the green and dark green bars in Fig. 9). Especially the CO₂ emissions of the fire seasons in 2006, 2007, 2008 and 2010 are smaller compared to GFED4s. The blue bars show the estimated emissions of the CarbonTracker XCO₂ enhancements using the STILT-based method. Here, similar emissions as compared to GFED4s are expected as CarbonTracker uses the fire CO₂ emissions of GFED4s as input. As shown by the large differences between the GFED4s and CarbonTracker based CO₂ emissions the estimation of the fire emissions in this region is more difficult than in North Africa. The reason can be an insufficient sampling of the satellite data as well as large uncertainties in the atmospheric transport in this region and these time periods. As a result the uncertainties of the satellite-based emissions are larger compared to the North Africa region.

Table 5 summarizes the found CO₂ emissions. The satellite-based CO₂ emissions are often smaller or similar compared to the emission inventory. The averaged emission and the standard deviation for the different methods show that the results of the STILT-based method (SM) are more variable (mean CO₂ emission: 518 ± 298 MtC) than the results of the CO₂-model based method (CM, mean CO₂ emission: 386 ± 173 MtC). The reason for this can be larger uncertainties in the atmospheric transport performed by STILT compared to the more complex CO₂ model CarbonTracker. Overall, the estimated emission for all years using both methods is 452 ± 244 MtC, which is about 36 % smaller compared to GFED4s.

The error analysis for the estimated fire CO₂ emissions has been performed in the same manner as for the Indonesian fire in 2015 and the fire seasons in North Africa. The results of this analysis have been summarized in Tab. 6 for the fire season in 2003. The overall uncertainty is in this time period for the STILT-based method about 33 % (1σ) and for the CO₂ model-based method about 38 % (1σ).

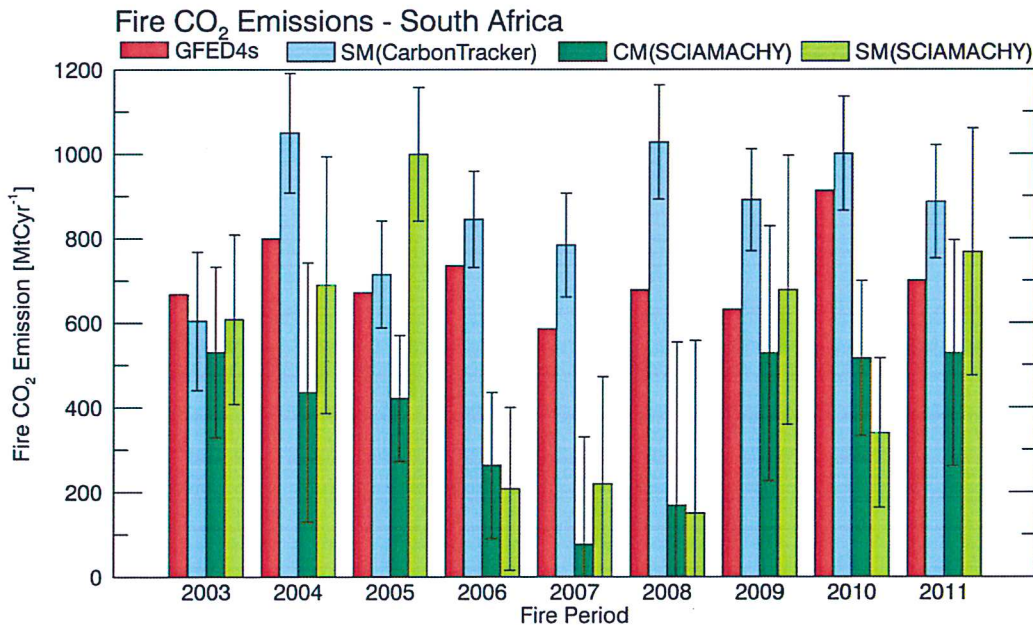


Figure 9. Estimated CO₂ emissions for fire seasons in 2003 to 2011 in South Africa based on SCIAMACHY BESD (green, dark green) compared to the GFED4s (red). The SCIAMACHY emissions are obtained by using the STILT-based method (SM, shown in green) and by using the CO₂ model based method (CM, shown in dark green). The emissions shown in blue are obtained by using the STILT-based method for the CO₂ model fire enhancements.

Fire season	CO ₂ Emission [MtC]			
	GFED4s	SM	CM	Mean
2003	668	608±200	530±202	569±201
2004	800	690±304	436±306	563±305
2005	672	999±159	421±149	710±154
2006	736	208±192	263±172	236±183
2007	586	220±253	77±253	149±253
2008	679	150±408	169±385	160±397
2009	632	678±318	528±301	603±310
2010	913	340±177	516±183	428±180
2011	701	768±293	529±267	648±280
Mean	709±97	518±298	386±173	452±244

Table 5. Estimated CO₂ emissions for the fire seasons in South Africa. The SCIAMACHY BESD based emissions are obtained by using the STILT-based method (SM) and the CO₂ model-based method (CM). Mean values and their standard deviation for all fire seasons are shown in the bottom. The mean values on the right are the means of the SM and CM based emissions.

Error Contribution	SM		CM	
	Systematic	Statistical	Systematic	Statistical
Data and GFASv1.2 uncertainty	-	0.118	-	0.120
Background, sampling, atmospheric transport	0.095	0.245	0.095	0.245
Aerosols	0.024	-	0.028	-
Albedo	0.009	-	0.009	-
All	0.128	0.271	0.120	0.272
Overall	0.300 (33.0 %)		0.302 (38.1 %)	

Table 6. Error analysis results for the scaling factor obtained by using the STILT-based estimation method (SM) and the CO₂ model-based estimation method (CM) for the South African fire season in 2003.

4.2.3 South America

The SCIAMACHY XCO₂ data (XCO₂^{obs}), the used background concentrations (XCO₂^{back}) and the XCO₂ enhancements (XCO₂^{fire}) for South America averaged over the fire seasons between 2003 (April - October) and 2011 are shown in Fig. 10. The spatial distribution of the satellite observations shows that the subtraction of the background concentration from the SCIAMACHY XCO₂ results in XCO₂ enhancements of up to 7 ppm.

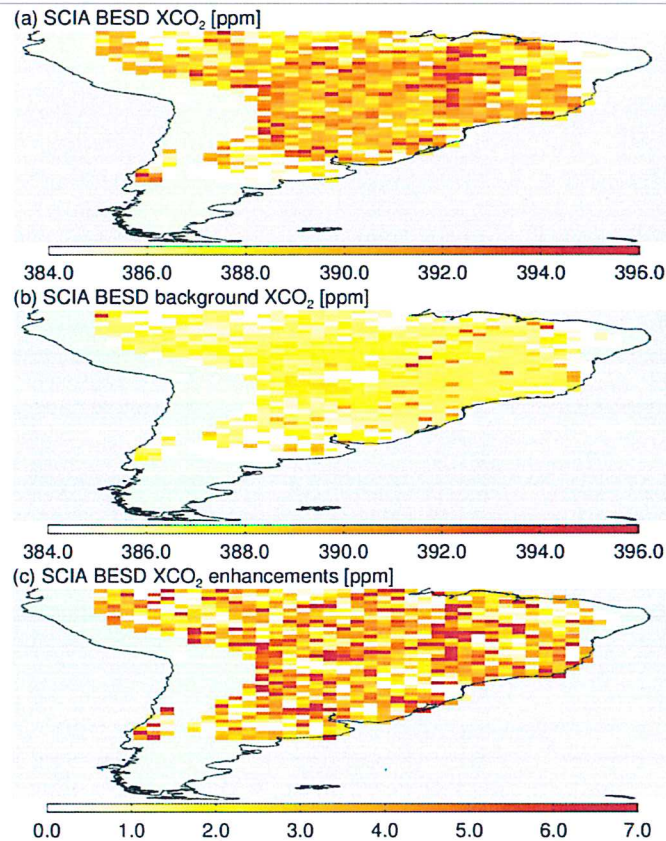


Figure 10. (a) SCIAMACHY BESD XCO_2 , (b) corresponding background XCO_2 , and (c) XCO_2 enhancements on a $1^\circ \times 1^\circ$ grid for South America and averaged over the fire seasons 2003 to 2011.

The SCIAMACHY measurements, which are not influenced by fire CO_2 emissions, have been identified by small fire influences ($XCO_2^{\text{fire, STILT}} < 0.01$ ppm). The SCIAMACHY data and the corresponding fire influences have been gridded on daily $1^\circ \times 1^\circ$ grids (see e.g. Fig. 6 for SCIAMACHY XCO_2 , background XCO_2 and the resulting XCO_2 enhancements) to reduce the scatter of the satellite data and to reduce potential errors resulting from the atmospheric transport simulations. The bounding box around the investigated area covers the latitude range between -55° and 0° , and the longitude range between -82° and -33° .

Figure 11 shows the estimated fire CO_2 emissions based on the CO_2 model-based method and the STILT-based method. The satellite-based CO_2 emissions are similar compared to the GFED4s emissions (shown by the green and dark green bars in Fig. 11). The blue bars show the estimated emissions of the CarbonTracker XCO_2 enhancements using the STILT-based method. As shown by the large differences between the GFED4s and CarbonTracker based CO_2 emissions the estimation of the fire emissions in this region is difficult, especially in the year 2010. The reason can be an insufficient sampling and limited amount of satellite data as well as large uncertainties in the atmospheric transport in this region and this time period. As a result the uncertainties of the satellite-based emissions are larger compared to other time periods.

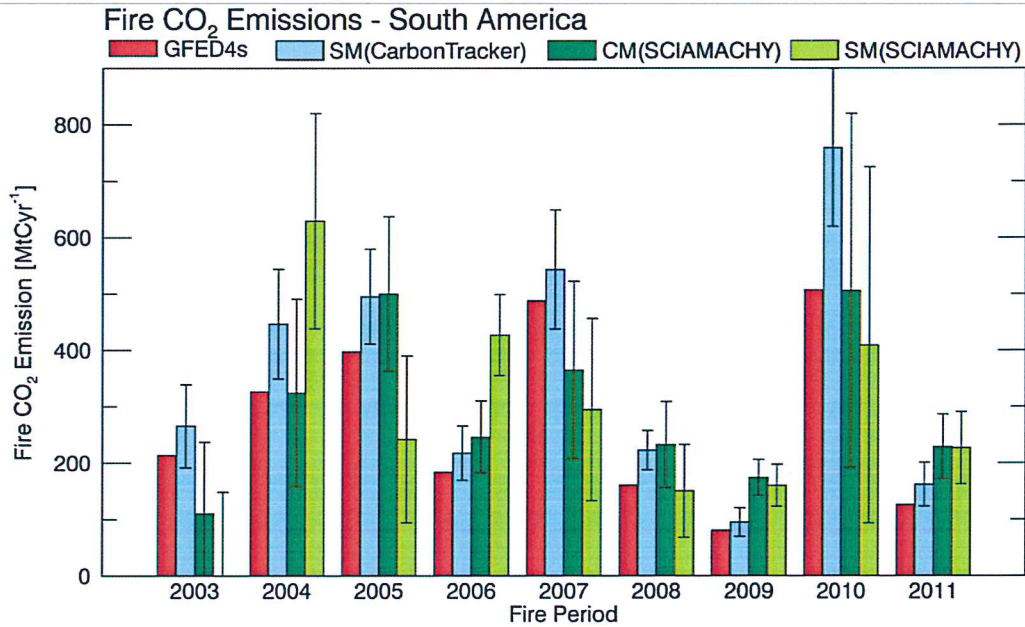


Figure 11. Estimated CO₂ emissions for the fire seasons in 2003 to 2011 in South America based on SCIAMACHY BESD (green, dark green) compared to GFED4s (red). The SCIAMACHY emissions are obtained by using the STILT-based method (SM, shown in green) and by using the CO₂ model-based method (CM, shown in dark green). The emissions shown in blue are obtained by using the STILT-based method for the CO₂ model fire enhancements.

Table 7 summarizes the found CO₂ emissions. The averaged emission and the standard deviation for the different methods are similar (Stilt-based method, mean CO₂ emission: 279±190 MtC; CO₂-model based method, mean CO₂ emission: 298±138 MtC). Overall, the estimated emission for all years using both methods is 289±143 MtC, which is very similar to the fire CO₂ emission in GFED4s.

The error analysis for the estimated fire CO₂ emissions has been performed in the same manner as for the Indonesian fires in 2015 and the fire seasons in North and South Africa. The results of this analysis have been summarized in Tab. 8 for the fire season in 2004. The overall uncertainty is in this time period for the STILT-based method about 30 % (1σ) and for the CO₂ model-based method about 51 % (1σ).

Fire season	CO ₂ Emission [MtC]			
	GFED4s	SM	CM	Mean
2003	214	-27±176	110±127	42±153
2004	326	629±191	324±167	477±179
2005	397	242±148	500±137	371±143
2006	184	427±72	246±64	336±68
2007	488	294±161	365±157	330±159
2008	160	150±82	232±77	191±80
2009	81	160±38	174±32	167±35
2010	507	409±316	506±314	457±315
2011	126	227±64	229±58	228±61
Mean	276±157	279±190	298±138	289±143

Table 7. Estimated CO₂ emissions for the fire seasons in South America. The SCIAMACHY BESD based emissions are obtained by using the STILT-based method (SM) and the CO₂ model-based method (CM). Mean values and their standard deviation for all fire seasons are shown in the bottom. The mean values on the right are the means of the SM and CM based emissions.

Error Contribution	SM		CM	
	Systematic	Statistical	Systematic	Statistical
Data and uncertainty	-	0.249	-	0.125
Background, sampling, atmospheric transport	0.377	0.299	0.377	0.299
Aerosols	0.036	-	0.009	-
Albedo	0.032	-	0.017	-
All	0.437	0.389	0.394	0.324
Overall	0.585 (30.3 %)		0.510 (51.3 %)	

Table 8. Error analysis results for the scaling factor obtained by using the STILT-based estimation method (SM) and the CO₂ model-based estimation method (CM) for the South American fire season in 2004.

5 Conclusions

Within ESA's Living Planet Fellowship project CARBOn dioxide emissions from FIRES (CARBOFIRES) CO₂ emissions of fires have been estimated by using satellite-derived CO₂ concentrations. The CO₂ emissions of the Indonesian fires in 2015 and the fire seasons in North and South Africa and South America were estimated. Column-averaged dry air mole fractions of CO₂, XCO₂, data product retrieved from observations of NASA's Orbiting Carbon Observatory-2 (OCO-2) mission and from observations of the SCanning Imaging Absorption spectroMeter for Atmospheric CHartography (SCIAMACHY) on-board the European Space Agency's (ESA) ENVironmental SATellite (ENVISAT) have been used. To estimate the fire CO₂ emissions, atmospheric transport simulations have been performed by using the Stochastic Time-Inverted Lagrangian Transport model, STILT, to identify satellite data affected by fires. These simulations have been used to determine the fire related XCO₂ enhancements in the satellite data by estimating the XCO₂ for fire free conditions. The fire CO₂ emission was subsequently estimated from the satellite XCO₂ enhancements by comparison with modelled XCO₂ enhancements (CO₂ model-based estimation method) and STILT model output (STILT-based estimation method).

The impact of various error sources such as aerosol related biases in the satellite data has been analyzed. In addition, uncertainties of the CO₂ emission databases have been included in the analysis to account for uncertainties related to the emission estimate and the knowledge of the spatial pattern in the databases. This is needed because the CO₂ model-based and STILT-based estimation methods depend on this pattern.

The analysis regarding the Indonesian fires in 2015 resulted in an OCO-2-based CO₂ fire emission of on average 748±206 MtCO₂ for the period from July to November 2015 which is about 35% and 30% lower than the estimate by the Global Fire Assimilation System (GFASv1.2: 1157 MtCO₂) and the Global Fire Emission Database (GFED4s: 1064 MtCO₂), respectively. These results are more consistent with the result of Huijnen et al. [2016] who also found lower emissions (27% lower than GFASv1.2 and 19% lower than GFED4s) as compared to the fire emission databases but for the period from September to October 2015.

The analysis concerning the CO₂ emissions of the fire seasons in North and South Africa and South America were performed using the SCIAMACHY BESD XCO₂ dataset [Reuter et al., 2010; Reuter et al., 2011] for the time period from 2003 to 2011. The results for the North Africa fire seasons show that the CO₂ emission is about 3,032±1,144 MtCO₂ (827±312 MtC) averaged over all years, which is about 96% larger as compared to GFED4s (1,547±257 MtCO₂; 422±70 MtC). The estimated fire CO₂ emission in South Africa is about 1,657±895 MtCO₂ (452±244 MtC) on average, which is about 36% smaller compared to GFED4s (2,600±356 MtCO₂; 709±97 MtC). The sum of the satellite-based African fire CO₂ emissions, North and South Africa together, are similar to the African fire CO₂ emissions in GFED4s. This can be an indication for an erroneous spatial distribution of the CO₂ emissions in the inventory. The South American fire CO₂ emission is on average about 1,060±524 MtCO₂ (289±143 MtC), which is similar to the fire CO₂ emission in GFED4s (1,012±576; 276±157 MtC).

These results have implication for global CO₂ flux inversions as it is currently not possible to constrain CO₂ fire emissions. The reason for this is the sparseness of atmospheric input data (e.g., CO₂ measurements performed by air sampling networks) and the fact that the influence of fires in the atmospheric CO₂ concentration is smaller than the spatiotemporal variability caused by the vegetation fluxes. As a result, pyrogenic CO₂

emissions are estimated from bottom-up inventories alone and any overestimation or underestimation is erroneously aliased into fluxes from other sources that are being optimized.

The methods developed in the CARBOFIRES project can be applied to other potentially interesting fire events. Furthermore, it is expected that the use of other satellite instruments like GOSAT and data from different XCO₂ retrieval algorithms will improve the estimation of CO₂ emissions from vegetation fires in the near future.

6 List of peer-reviewed publications related to the CARBOFIRES project (chronological)

Heymann, J., M. Reuter, M. Hilker, M. Buchwitz, O. Schneising, H. Bovensmann, J. P. Burrows, A. Kuze, H. Suto, N. M. Deutscher, M. K. Dubey, D. W. T. Griffith, F. Hase, S. Kawakami, R. Kivi, I. Morino, C. Petri, C. Roehl, M. Schneider, V. Sherlock, R. Sussmann, V. A. Velazco, T. Warneke, and D. Wunch, Consistent satellite XCO₂ retrievals from SCIAMACHY and GOSAT using the BESD algorithm, *Atmos. Meas. Tech.*, 8, 2961-2980, 2015.

Reuter, M., M. Buchwitz, M. Hilker, J. Heymann, H. Bovensmann, J. Burrows, S. Houweling, Y. Liu, R. Nassar, F. Chevallier, P. Ciais, J. Marshall, and M. Reichstein, How much CO₂ is taken up by the European terrestrial biosphere? *Bull. Amer. Meteor. Soc.* doi:10.1175/BAMS-D-15-00310.1, in press, 2016.

Massart, S., A. Agusti-Panareda, J. Heymann, M. Buchwitz, F. Chevallier, M. Reuter, M. Hilker, J. P. Burrows, N. M. Deutscher, D. G. Feist, F. Hase, R. Sussmann, F. Desmet, M. K. Dubey, D. W. T. Griffith, R. Kivi, C. Petri, M. Schneider, V. A. Velazco, Ability of the 4-D-Var analysis of the GOSAT BESD XCO₂ retrievals to characterize atmospheric CO₂ at large and synoptic scales, *Atmos. Chem. Phys.*, 16, 1653-1671, doi:10.5194/acp-16-1653-2016, 2016.

Buchwitz, M., M. Reuter, O. Schneising, W. Hewson, R.G. Detmers, H. Boesch, O.P. Hasekamp, I. Aben, H. Bovensmann, J.P. Burrows, A. Butz, F. Chevallier, B. Dils, C. Frankenberg, J. Heymann, G. Lichtenberg, M. De Mazière, J. Notholt, R. Parker, T. Warneke, C. Zehner, D.W.T. Griffith, N.M. Deutscher, A. Kuze, H. Suto, D. Wunch, Global satellite observations of column-averaged carbon dioxide and methane: The GHG-CCI XCO₂ and XCH₄ CRDP3 data set, *Remote Sensing of Environment*, DOI: 10.1016/j.rse.2016.12.027, <http://dx.doi.org/10.1016/j.rse.2016.12.027>, in press, pp. 20, 2016.

Heymann, J., M. Reuter, M. Buchwitz, O. Schneising, H. Bovensmann, J. P. Burrows, S. Massart, J. W. Kaiser, and D. Crisp, CO₂ emission of Indonesian fires in 2015 estimated from satellite-derived atmospheric CO₂ concentrations, *Geophys. Res. Lett.*, 44, doi:10.1002/2016GL072042, 2017.

7 Acknowledgements

M. Buchwitz, M. Reuter and O. Schneising from the GHG-CCI project as well as H. Bovensmann, J. P. Burrows, S. Massart, J. W. Kaiser and D. Crisp have contributed to these results. NASA has made available the OCO-2 XCO₂ L2 data products and ECMWF the meteorological, GFAS, and CO₂ analysis data sets. The CarbonTracker results have been obtained from NOAA ESRL, Boulder, Colorado, USA, from the website at <http://carbontracker.noaa.gov>. The Global Fire Emissions Database (GFED) version 4s has been obtained from <http://www.globalfiredata.org>.

8 References

Archibald, S., Staver, C., and Levin, S. A.: Evolution of human-driven fire regimes in Africa, *P. Natl. Acad. Sci. USA*, 109, 847–852. 2012.

Berrisford, P., Dee, D., Poli, P., Brugge, R., Fielding, K., Fuentes, M., Källberg, P. W., Kobayashi, S., Uppala, S., and Simmons, A., The ERA-Interim archive Version 2.0, ERA Report Series 1, ECMWF, Shinfield Park, Reading, UK, 13177, 2011.

Bovensmann, H. Burrows, J. P., Buchwitz, M., Frerick, J., Noël, S., Rozanov, V. V., Chance, K. V., and Goede, A.: SCIAMACHY – mission objectives and measurement modes, *J. Atmos. Sci.*, 56, 127 – 150, 1999.

Bowman, D. M. J. S., Balch, J. K., Artaxo, P., Bond, W. J., Carlson, J. M., Cochrane, M. A., D’Antonio, C. M., DeFries, R. S., Doyle, J. C., Harrison, S. P., Johnston, F. H., Keeley, J. E., Krawchuk, M. A., Kull, C. A., Marston, J.

B., Moritz, M. A., Prentice, I. C., Roos, C. I., Scott, A. C., Swetnam, T. W., van der Werf, G. R., and Pyne, S. J.: Fire in the Earth System, *Science*, 324, 481–484, doi:10.1126/science.1163886, 2009.

Buchwitz, M., Reuter, R., Schneising, O., Bösch, H., Guerlet, S., Dils, B., Aben, I., Armante, R., Bergamaschi, P., Blumenstock, T., Bovensmann, H., Brunner, D., Buchmann, B., Burrows, J. P., Butz, A., Chedin, A., Chevallier, F., Crevoisier, C. D., Deutscher, N. M., Frankenberg, C., Hase, F., Hasekamp, O. P., Heymann, J., Kaminski, T., Laeng, A., Lichtenberg, G., De Maziere, M., Noel, S., Notholt, J., Orphal, J., Popp, C., Parker, R., Scholze, M., Sussmann, R., Stiller, G. P., Warneke, T., Zehner, C., Bril, A., Crisp, D., Griffith, D. W. T., Kuze, A., O'Dell, D. W. T., Oshchepkov, S., Sherlock, V., Suto, H., Wennberg, P., Wunch, D., Yokota, T., and Yoshida, Y.: The Greenhouse Gas Climate Change Initiative (GHG-CCI): comparison and quality assessment of near-surface-sensitive satellite derived CO₂ and CH₄ global data sets, *Remote Sens. Environ.*, 162, 334-362, doi:10.1016/j.rse.2013.04.024, 2015.

Burrows, J. P., Hölzle, E., Goede, A. P. H., Visser, H., and Fricke, W.: SCIAMACHY – Scanning Imaging Absorption Spectrometer for Atmospheric Cartography, *Acta Astronaut.*, 35, 445 – 451, 1995.

Canadell, J. G., Le Quéré, C., Raupach, M. R., Field, C. B., Buitenhuis, E. T., Ciais, P., Conway, T. J., Gillet, N. P., Houghton, R. A., and Marland, G.: Contributions to accelerating atmospheric CO₂ growth from economic activity, carbon intensity, and efficiency of natural sinks, *Proceedings of the National Academy of Sciences (PNAS) of the United States of America*, November 20, 2007, 104, 18866 – 18870, 2007.

Crisp, D., Miller, C. E., and DeCola, P. L., NASA Orbiting Carbon Observatory: measuring the column averaged carbon dioxide mole fraction from space, *J. Appl. Remote Sens.*, 2(1), 023508, doi:10.1117/1.2898457, 2008.

Crisp, D., Fisher, B. M., O'Dell, C., Frankenberg, C., Basilio, R., Bösch, H., Brown, L. R., Castano, R., Connor, B., Deutscher, N. M., Eldering, A., Griffith, D., Gunson, M., Kuze, A., Mandrake, L., McDuffie, J., Messerschmidt, J., Miller, C. E., Morino, I., Natraj, V., Notholt, J., O'Brien, D. M., Oyafuso, F., Polonsky, I., Robinson, J., Salawitch, R., Sherlock, V., Smyth, M., Suto, H., Taylor, T. E., Thompson, D. R., Wennberg, P. O., Wunch, D., and Yung, Y. L., The ACOS CO₂ retrieval algorithm – Part II: Global XCO₂ data characterization, *Atmos. Meas. Tech.*, 5, 687-707, doi:10.5194/amt-5-687-2012, 2012.

Crisp, D., Measuring atmospheric carbon dioxide from space with the Orbiting Carbon Observatory-2 (OCO-2), *Proc. SPIE 9607, Earth Observing Systems XX*, 960702, doi:10.1117/12.2187291, 2015.

Dils, B., Buchwitz, M., Reuter, M., Schneising, O., Boesch, H., Parker, R., Guerlet, S., Aben, I., Blumenstock, T., Burrows, J. P., Butz, A., Deutscher, N. M., Frankenberg, C., Hase, F., Hasekamp, O. P., Heymann, J., De Mazière, M., Notholt, J., Sussmann, R., Warneke, T., Griffith, D., Sherlock, V., and Wunch, D.: The Greenhouse Gas Climate Change Initiative (GHG-CCI): comparative validation of GHG-CCI SCIAMACHY/ENVISAT and TANSO-FTS/GOSAT CO₂ and CH₄ retrieval algorithm products with measurements from the TCCON, *Atmos. Meas. Tech.*, 7, 1723–1744, doi:10.5194/amt-7-1723-2014, 2014.

Duncan, B. N., Martin, R. V., Staudt, A. C., Yevich, R., and Logan, J. A.: Interannual and seasonal variability of biomass burning emissions constrained by satellite observations, *J. Geophys. Res.-Atmos.*, 108, 4100, doi:10.1029/2002JD002378, 2003.

Field, R.D., Shen, S. S. P., Predictability of carbon emissions from biomass burning in Indonesia from 1997 to 2006, *J. Geophys. Res.*, 113, G04024, doi: 10.1029/2008JG000694, 2008.

Gerbig, C., Lin, J. C., Wofsy, S.C., Daube, B. C., Andrews, A. E., Stephens, B. B., Bakwin, P. S., and Grainger, C. A., Toward constraining regional-scale fluxes of CO₂ with atmospheric observations over a continent: 2. Analysis of COBRA data using a receptor-oriented framework, *J. Geophys. Res.-Atmos.*, 108, 4757, doi:10.1029/2003JD003770, 2003.

Guyon, P., Frank, G. P., Welling, M., Chand, D., Artaxo, P., Rizzo, L., Nishioka, G., Kolle, O., Fritsch, H., Silva Dias, M. A., F., Gatti, L. V., Cordova, A. M., and Andreae, M. O., Airborne measurements of trace gas and aerosol particle emissions from biomass burning in Amazonia, *Atmos. Chem. Phys.*, 5, 2989 – 3002, doi:10.5194/acp-5-2989-2005, 2005.

Heymann, J., Reuter, M., Hilker, M., Buchwitz, M., Schneising, O., Bovensmann, H., Burrows, J. P., Kuze, A., Suto, H., Deutscher, N. M., Dubey, M. K., Griffith, D. W. T., Hase, F., Kawakami, S., Kivi, R., Morino, I., Petri, C., Roehl, C., Schneider, M., Sherlock, V., Sussmann, R., Velazco, V. A., Warneke, T., and Wunch, D., Consistent satellite XCO₂ retrievals from SCIAMACHY and GOSAT using the BESD algorithm, *Atmos. Meas. Tech.*, 8, 2961–2980, doi:10.5194/amt-8-2961-2015, 2015.

Heymann, J., M. Reuter, M. Buchwitz, O. Schneising, H. Bovensmann, J. P. Burrows, S. Massart, J. W. Kaiser, and D. Crisp, CO₂ emission of Indonesian fires in 2015 estimated from satellite-derived atmospheric CO₂ concentrations, *Geophys. Res. Lett.*, 44, doi:10.1002/2016GL072042, 2017.

Hollmann, R., Merchant, C. J., Saunders, R., Downy, C., Buchwitz, M., Cazenave, A., Chuvieco, E., Defourny, P., de Leeuw, G., Forsberg, R., Holzer-Popp, T., Paul, F., Sandven, S., Sathyendranath, S., van Roozendaal, M., and Wagner, W.: The ESA climate change initiative: satellite data records for essential climate variables, *B. Am. Meteorol. Soc.*, 94, 1541–1552, doi:10.1175/BAMS-D-11-00254.1, 2013.

Huijnen, V., Wooster, M. J., Kaiser, J. W., Gaveau, D. L. A., Flemming, J., Parrington, M., Inness, A., Murdiyarso, D., Main, B., and van Weele, M., Fire carbon emissions over maritime southeast Asia in 2015 largest since 1997, *Scientific Reports*, 6, 26886, doi: 10.1038/srep26886, 2016.

IPCC: Climate Change 2007: The Physical Science Basis, contribution of Working Group I to the Fourth Assessment Report of the Intergovernmental Panel on Climate Change, edited by: Solomon, S., Qin, D., Manning, M., Chen, Z., Marquis, M., Averyt, K. B., Tignor, M., and Miller, H. L., Cambridge Univ. Press, Cambridge, UK and New York, USA, 2007.

Kaiser, J. W., Heil, A., Andreae, M. O., Benedetti, A., Chubarova, N., Jones, L., Morcrette, J.-J., Razinger, M., Schultz, M. G., Suttie, M., and van der Werf, G. R., Biomass burning emissions estimated with a global fire assimilation system based on observed fire radiative power, *Biogeosciences*, 9, 527–554, doi:10.5194/bg-9-527-2012, 2012.

Kaiser, J. W., van der Werf, G. R., and Heil, A., [Global climate] Biomass burning [in “State of the Climate in 2015”], *Bull. Amer. Meteor. Soc.*, 97 (8), S60-S62, 2016.

Lin, J. C., Gerbig, C., Wofsy, S. C., Andrews, A. E., Daube, B. C., Davis, K. J., and Grainger, C. A., A near-field tool for simulating the upstream influence of atmospheric observations: The Stochastic Time-Inverted Lagrangian Transport (STILT) model, *J. Geophys. Res.-Atmos.*, 108, 4493, doi:10.1029/2002JD003161, 2003.

Marlier, M. E., DeFries R. S., Voulgarakis, A., Kinney, P. L., Randerson, J. T., Shindell, D. T., Chen, Y., and Faluvegi, G., El Niño and health risks from landscape fire emissions in southeast Asia, *Nature Climate Change*, 3, 131-136, doi:10.1038/nclimate1658, 2013.

Massart, S., Agustí-Panareda, A., Heymann, J., Buchwitz, M., Chevallier, F., Reuter, M., Hilker, M., Burrows, J. P., Deutscher, N. M., Feist, D. G., Hase, F., Sussmann, R., Desmet, F., Dubey, M. K., Griffith, D. W. T., Kivi, R., Petri, C., Schneider, M., and Velazco, V. A., Ability of the 4-D-Var analysis of the GOSAT BESD XCO₂ retrievals to characterize atmospheric CO₂ at large and synoptic scales, *Atmos. Chem. Phys.*, 16, 1653-1671, doi:10.5194/acp-16-1653-2016, 2016.

O'Dell, C. W., Connor, B., Bösch, H., O'Brien, D., Frankenberg, C., Castano, R., Christi, M., Eldering, D., Fisher, B., Gunson, M., McDuffie, J., Miller, C. E., Natraj, V., Oyafuso, F., Polonsky, I., Smyth, M., Taylor, T., Toon, G. C., Wennberg, P. O., and Wunch, D., The ACOS CO₂ retrieval algorithm – Part 1: Description and validation against synthetic observations, *Atmos. Meas. Tech.*, 5, 99-121, doi:10.5194/amt-5-99-2012, 2012.

O’Shea, S. J., Allen, G., Gallagher, M. W., Bauguitte, S. J.-B., Illingworth, S. M., Le Breton, M., Muller, J. B. A., Percival, C. J., Archibald, A. T., Oram, D. E., Parrington, M., Palmer, P. I., and Lewis, A. C., Airborne observation of trace gases over boreal Canada during BORTAS: campaign climatology, air mass analysis and enhancement ratios, *Atmos. Chem. Phys.*, 13, 12451 – 12467, 2013.

Peters, W., Jacobson, A. R., Sweeney, C., Andrews, A. E., Conway, T. J., Masarie, K., Miller, J. B., Bruhwiler, L. M.

P., Petron, G., Hirsch, A. I., Worthy, D. E. J., van der Werf, G. R., Randerson, J. T., Wennberg, P. O., Krol, M. C., and Tans, P. P., An atmospheric perspective on North American carbon dioxide exchange: CarbonTracker, *P. Natl. Acad. Sci. USA*, 104, 18925–18930, doi:10.1073/pnas.0708986104, 2007.

Reuter, M., Buchwitz, M., Schneising, O., Heymann, J., Bovensmann, H., and Burrows, J. P.: A method for improved SCIAMACHY CO₂ retrieval in the presence of optically thin clouds, *Atmos. Meas. Tech.*, 3, 209–232, doi:10.5194/amt-3-209-2010, 2010.

Reuter, M., Bovensmann, H., Buchwitz, M., Burrows, J. P., Connor, B. J., Deutscher, N. M., Griffith, D. W. T., Heymann, J., Keppel-Aleks, G., Messerschmidt, J., Notholt, J., Petri, C., Robinson, J., Schneising, O., Sherlock, V., Velasco, V., Warneke, T., Wennberg, P. O., and Wunch, D.: Retrieval of atmospheric CO₂ with enhanced accuracy and precision from SCIAMACHY: Validation with FTS measurements and comparison with model results, *J. Geophys. Res.*, 116, D04301, doi:10.1029/2010JD015047, 2011.

Reuter, M., Buchwitz, M., Hilker, M., Heymann, J., Schneising, O., Pillai, D., Bovensmann, H., Burrows, J. P., Bösch, H., Parker, R., Butz, A., Hasekamp, O., O'Dell, C. W., Yoshida, Y., Gerbig, C., Nehr Korn, T., Deutscher, N. M., Warneke, T., Notholt, J., Hase, F., Kivi, R., Sussmann, R., Machida, T., Matsueda, H., and Sawa, Y., Satellite-inferred European carbon sink larger than expected, *Atmos. Chem. Phys.*, 14, 13739–13753, doi:10.5194/acp-14-13739-2014, 2014.

Reuter, M., Bovensmann, H., Buchwitz, M., Burrows, J. P., Heymann, J., Hilker, M., and Schneising, O.: Algorithm Theoretical Basis Document Version 4 – The Bremen Optimal Estimation DOAS (BESD) algorithm for the retrieval of XCO₂ – ESA Climate Change Initiative (CCI) for the Essential Climate Variable (ECV), University of Bremen, available at: <http://www.esa-ghg-cci.org> (last access: 26 February 2016), 2015.

Reuter, M., Hilker, M., Schneising, O., Buchwitz, M., Heymann, J.: Comprehensive Error Characterisation Report: BESD full-physics retrieval algorithm for XCO₂ – Version 2, University of Bremen, available at: <http://www.esa-ghg-cci.org> (last access: 26 February 2016), 2016.

Tacconi, L., Preventing fires and haze in Southeast Asia, *Nature Climate Change*, 6, 640–643, doi:10.1038/nclimate3008, 2016.

van der Werf, G. R., Randerson, J. T., Giglio, L., Collatz, G. J., Mu, M., Kasibhatla, P. S., Morton, D. C., DeFries, R. S., Jin, Y., and van Leeuwen, T. T., Global fire emissions and the contribution of deforestation, savanna, forest, agricultural, and peat fires (1997–2009), *Atmos. Chem. Phys.*, 10, 11707–11735, doi:10.5194/acp-10-11707-2010, 2010.

Wooster, M. J., Perry, G. L. W., and Zoumas, A., Fire, drought and El Niño relationships on Borneo (Southeast Asia) in the pre-MODIS era (1980–2000), *Biogeosciences*, 9, 317–340, doi:10.5194/bg-9-317-2012, 2012.